This journal is © The Royal Society of Chemistry 2023

Supporting Information

Temperature dependent tailoring of the pore structure based on MOF-derived carbon electrodes for electrochemical capacitors

Yuru Wang[a], Qing Zhang[a,b,*]

[a] Institutes of Physical Science and Information Technology, Anhui University, Hefei, 230601, China

[b] Anhui Graphene Engineering Research Center, Anhui University, Hefei, 230601, China

Email: zhangq@ahu.edu.cn

Table S1. Set-up of the treatment conditions: carbonization temperature and the dwelling time.

Carbonization	Dwelling time t		
temperature T	0.5 h	2 h	4 h
450 ℃	T450-t0.5	ZnO/C-T450-t2	
500 ℃	ZnO/C-T500-t0.5	ZnO/C-T500-t2	
570 ℃	ZnO/C-T570-t0.5	ZnO/C-T570-t2	ZnO/C-T570-t4
700 ℃	ZnO/C-T700-t0.5	ZnO/C-T700-t2	

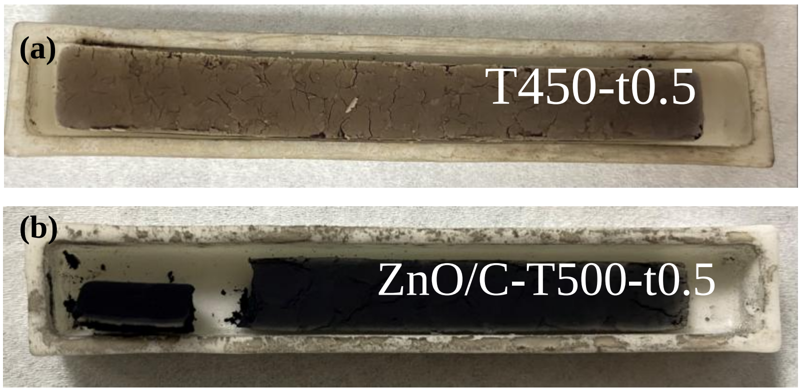

Fig. S1. The optical photographs of (a) T450-t0.5 showing brownish color, demonstrating that 450 ℃ was too low to produce well-carbonized material, while the rest showing black color, taking ZnO/C-T500-t0.5 (b) as an example.

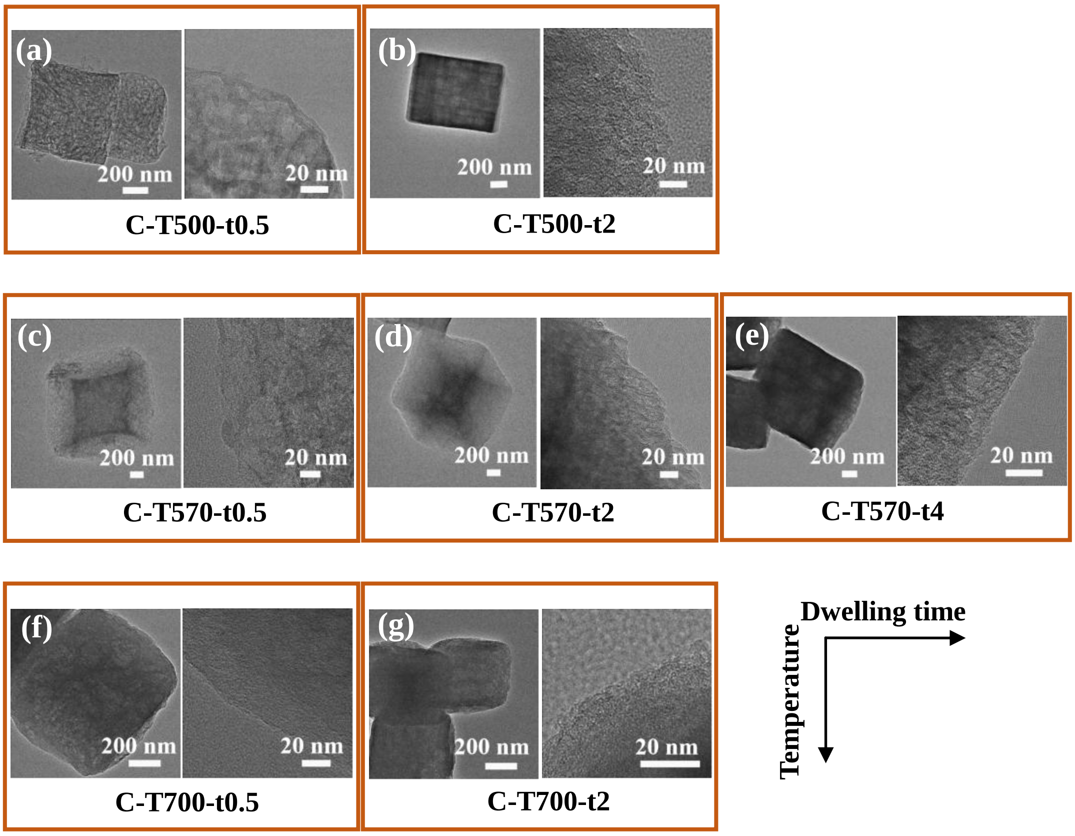

Fig. S2. TEM images of (a) C-T500-t0.5, (b) C-T500-t2, (c) C-T570-t0.5, (d) C-T570-t2, (e) C-T570-t4, (f) C-T700-t0.5, and (g) C-T700-t2, showing different sized pores.

The QSDFT (Quenched solid density functional theory) was selected to calculate the pore size distribution of our MOF-derived carbons in the range of pore widths from 0.4-35 nm from nitrogen at 77 K.

With selecting the calculation model as “N_2 at 77 K on carbon [slit/cylindr. pores, QSDFT]”, where the shape of the pores were consistent with the TEM and SEM characterization results, minimal fitting errors were obtained (Table S2 below), again demonstrating the applicability of the model. With controlling the “Interval” in “Interpolation ranges” to be 0.01 nm, pore size distribution data would be generated. The partial SSA and pore volume with respect to certain pore size range were calculated from the cumulative pore volume and cumulative surface area. For example, $SSA_{1\text{-}10\ nm}$ = cumulative SSA @ 10 nm – cumulative SSA @ 1nm, and $V_{1\text{-}10\ nm}$ = cumulative pore volume @ 10 nm – cumulative pore volume @ 1nm.

Table S2. The fitting errors as calculated using the QSDFT model.

Sample#	Fitting error (%)
C-T500-t0.5	0.425
C-T500-t2	0.226
C-T570-t0.5	0.315
C-T570-t2	0.223
C-T570-t4	0.209
C-T700-t0.5	0.453
C-T700-t2	0.155

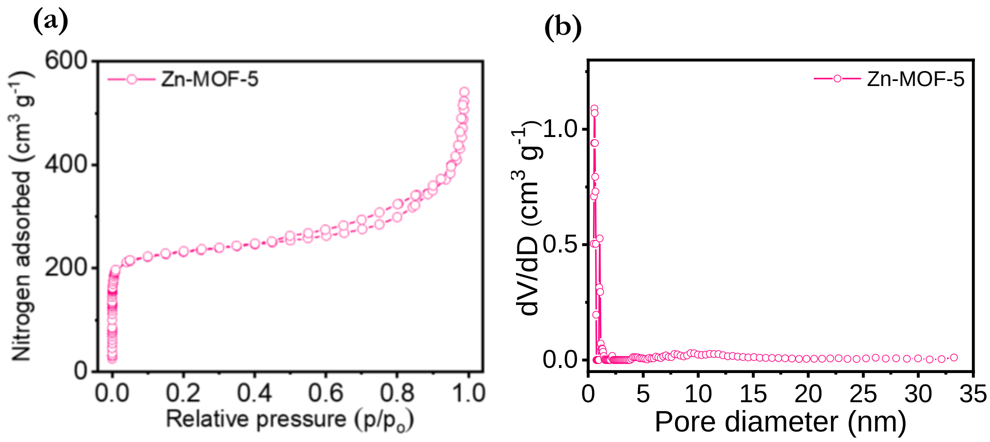

Fig. S3. (a) N_2 adsorption-desorption isotherms and (b) pore size distribution of Zn-MOF-5.

Table S3. The physical characteristics of Zn-MOF-5 and C-Tx-ty materials.

Sample#	SSA (m^2 g^{-1})	V_{total} (cm^3 g^{-1})	Avg. pore size (nm)
Zn-MOF-5	897	0.60	3.74
C-T500-t0.5	1689	2.84	7.80
C-T500-t2	1512	1.29	3.70
C-T570-t0.5	1794	2.69	7.20
C-T570-t2	1991	1.62	3.46
C-T570-t4	1585	1.27	3.37
C-T700-t0.5	1376	0.90	3.20
C-T700-t2	1832	1.36	4.00

Note: V_{total} is the total pore volume.

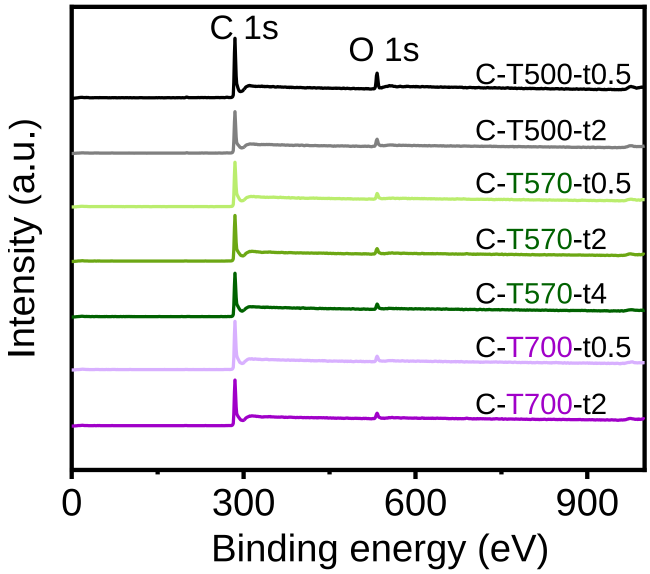

Fig. S4. XPS survey spectra of C-Tx-ty materials.

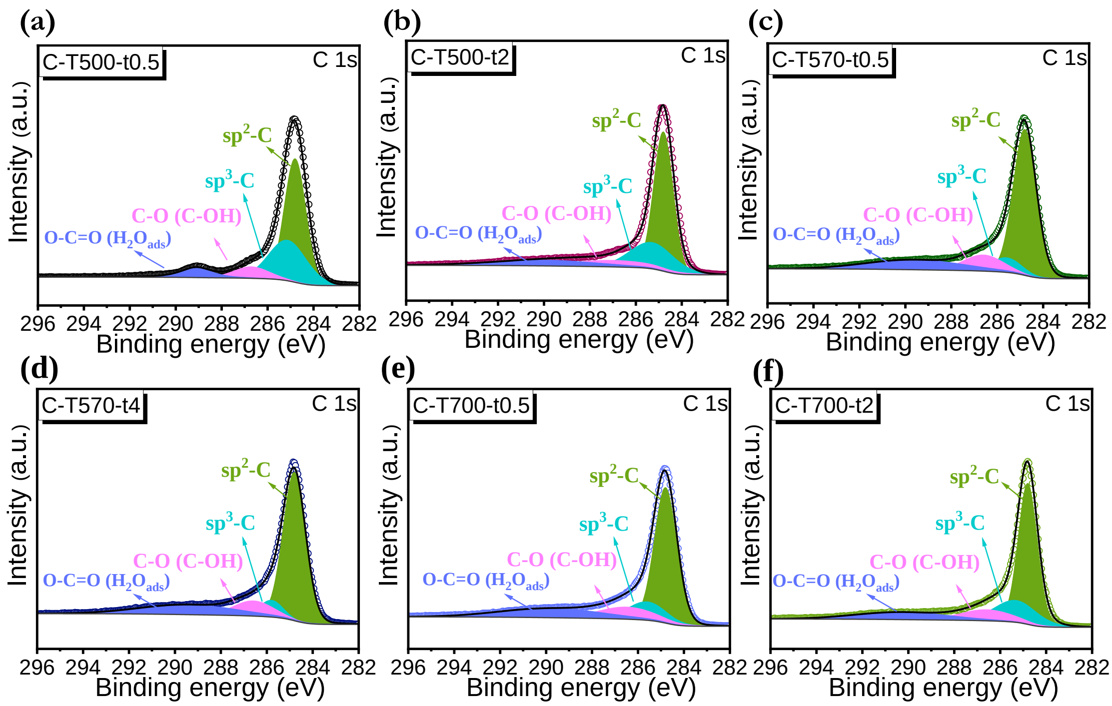

Fig. S5. High-resolution C 1s spectra of (a) C-T500-t0.5, (b) C-T500-t2, (c) C-T570-t0.5, (d) C-T570-t4, (e) C-T700-t0.5, and (f) C-T700-t2.

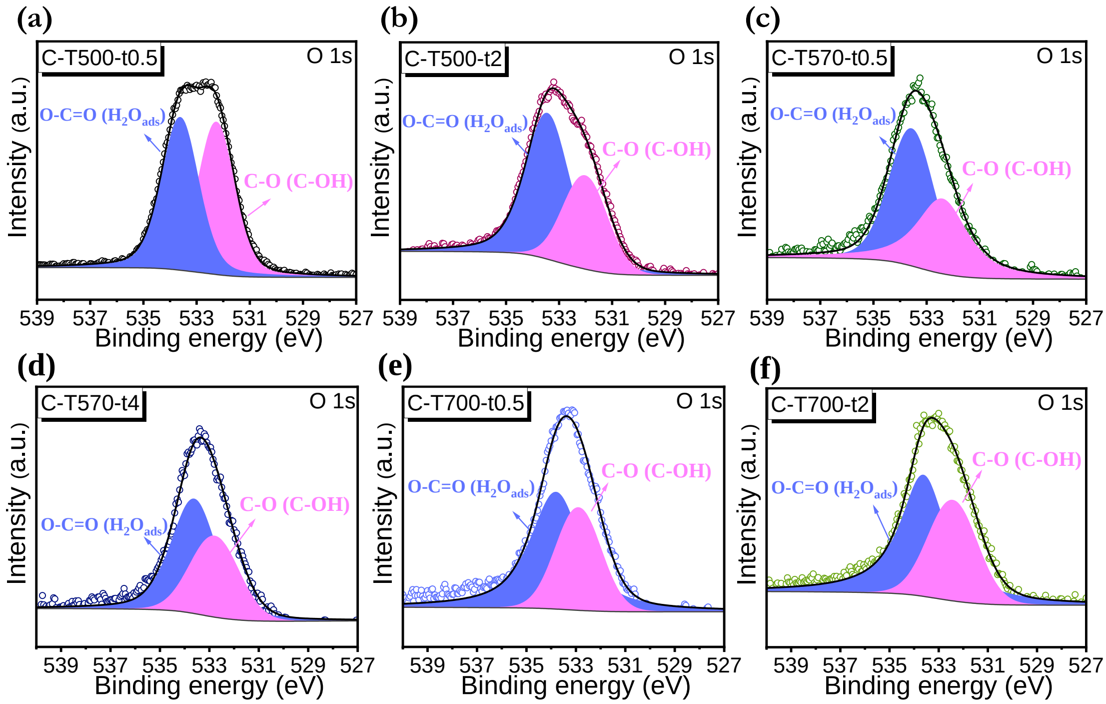

Fig. S6. High-resolution O 1s spectra of (a) C-T500-t0.5, (b) C-T500-t2, (c) C-T570-t0.5, (d) C-T570-t4, (e) C-T700-t0.5, and (f) C-T700-t2.

Table S4. XPS fitting results for for C-Tx-ty materials.

Sample#	at.%		C 1s (at.%)				O 1s (at.%)	
	C	O	sp^2-C	sp^3-C	C-O (C-OH)	O=C-O (H_2O_{ads})	C-O (C-OH)	O=C-O (H_2O_{ads})
C-T500-t0.5	89.4	10.6	52.62	30.83	8.23	8.32	49.24	50.76
C-T500-t2	92.1	7.9	53.33	22.43	9.85	14.39	34.52	65.48
C-T570-t0.5	94.1	5.9	63.79	7.78	11.24	17.19	43.08	56.92
C-T570-t2	93.7	6.3	65.47	11.19	6.32	17.02	32.50	67.50
C-T570-t4	94.5	5.5	64.98	6.98	10.74	17.30	38.51	61.49
C-T700-t0.5	94.4	5.6	57.98	12.64	12.22	17.16	35.96	64.04
C-T700-t2	94.1	5.9	56.99	18.17	11.19	13.65	37.36	62.64

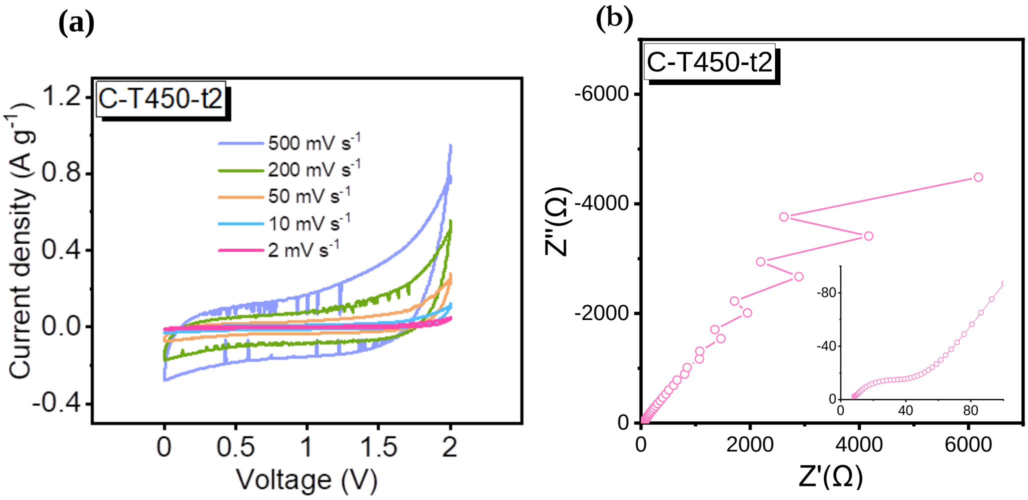

Fig. S7. CV curves and Nyquist plot of C-T450-t2, further demonstrating that 450 ℃ was too low to produce well-carbonized material even with prolonged dwelling time.

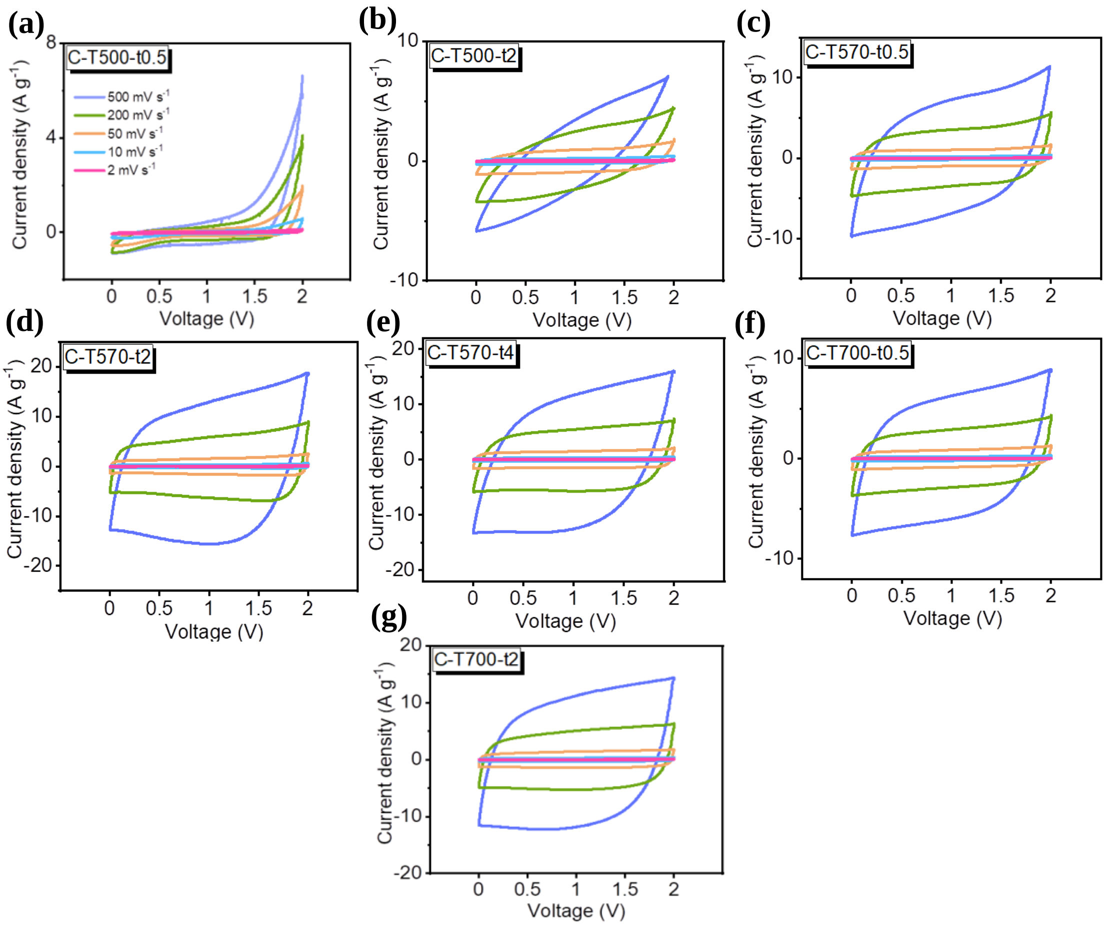

Fig. S8. (a-g) CV curves of C-Tx-ty under the scan rate from 2 to 500 mV s^{-1}.

Table S5. The specific capacitance values of C-Tx-ty at different scan rates and the capacitance retention at 500 mV s^{-1} as compared to 2 mV s^{-1}.

Sample#	500 (F g^{-1})	200 (F g^{-1})	50 (F g^{-1})	10 (F g^{-1})	2 (F g^{-1})	Rate capability (%)
C-T500-t0.5	2.1	3.7	8.3	18.8	30.0	7.0
C-T500-t2	15.1	18.4	32.5	42.8	47.3	31.9
C-T570-t0.5	32.1	44.4	52.8	58.4	64.2	50.0
C-T570-t2	48.1	56.2	68.9	72.7	79.9	60.2
C-T570-t4	43.4	52.1	59.4	64.6	69.9	62.1
C-T700-t0.5	27.9	33.5	41.1	49.2	56.7	49.3
C-T700-t2	39.3	48.6	56.7	61.7	70.3	55.9

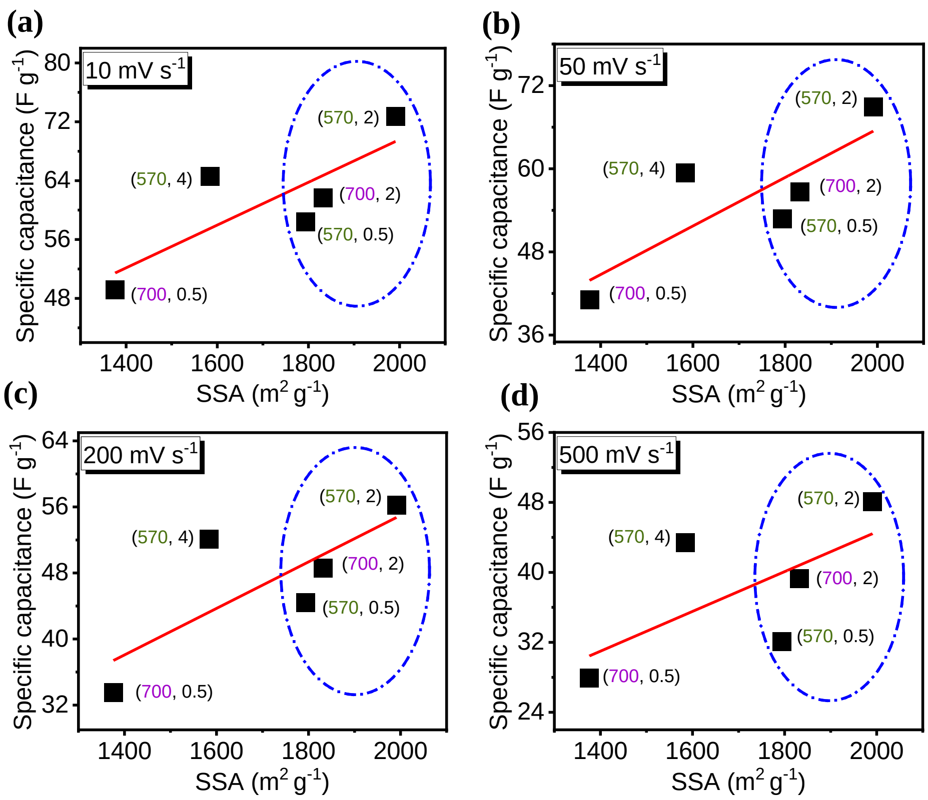

Fig. S9. Specific capacitance at the scan rate of (a) 10 mV s^{-1}, (b) 50 mV s^{-1}, (c) 200 mV s^{-1}, and (d) 500 mV s^{-1} versus the SSA of C-Tx-ty with the correlation coefficient R^2 ~0.65, 0.68, 0.60, and 0.44, respectively.

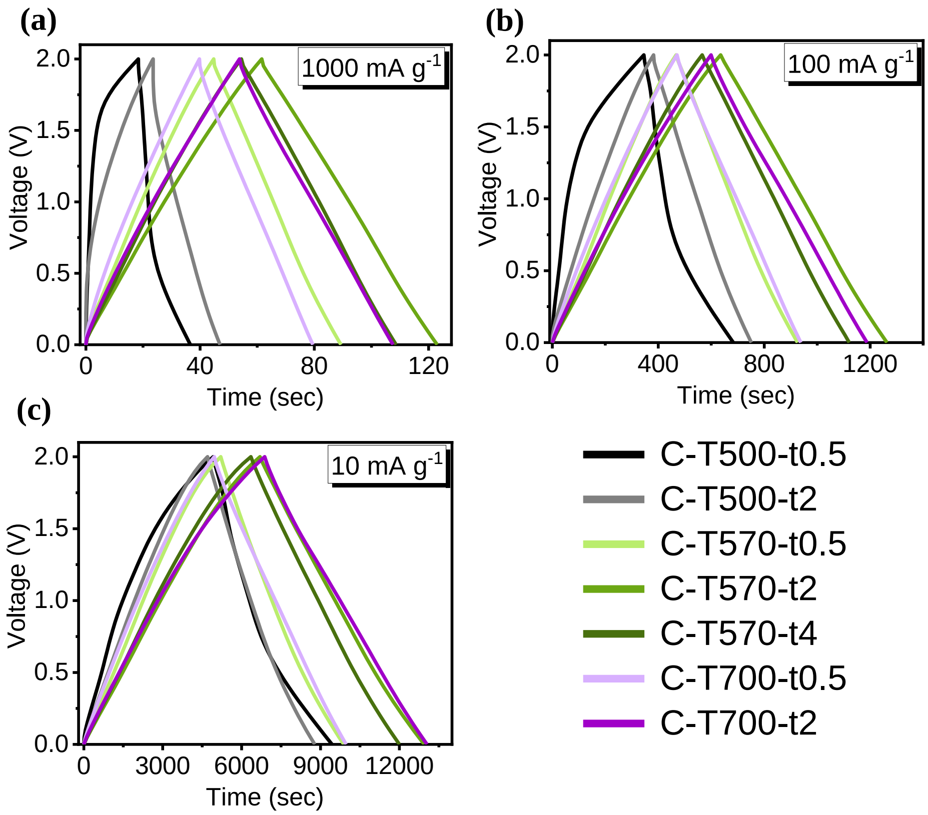

Fig. S10. Comparison of GCD curves of C-Tx-ty electrode materials with the current density of (a) 1000 mA g^{-1}, (b) 100 mA g^{-1}, and (c) 10 mA g^{-1}.

Fig. S10 presents that the GCD curves of the C-Tx-ty, except for C-T500-t0.5 and C-T500-t2. The curves showed equilateral triangles and no significant internal resistance drop, which further validated their good electrochemical double layer properties. In addition, their GCD curves were linear and symmetrical, indicating the high electrochemical reversibility. C-T500-t0.5 and C-T500-t2 leaded a shorter charge and discharge time among all C-Tx-ty electrode materials with the lowest specific capacitance values measured at three different current densities (listed in Table S6 below); while C-T570-t2 and C-T570-t4 with the highest ratio of medium pores admitted the highest specific capacitances. The results are consistent with CV results.

Table S6. Specific capacitance values of C-Tx-ty electrode materials obtained by GCD at current densities of 1000, 100 and 10 mA g^{-1}.

Sample#	Current density (mA g^{-1})	Specific capacitance (F g^{-1})
C-T500-t0.5	1000/100/10	18.2/33.8/45.2
C-T500-t2	1000/100/10	23.4/36.9/40.7
C-T570-t0.5	1000/100/10	44.5/45.9/46.8
C-T570-t2	1000/100/10	61.4/62.8/62.5
C-T570-t4	1000/100/10	54.2/55.5/56.5
C-T700-t0.5	1000/100/10	39.7/46.7/50.1
C-T700-t2	1000/100/10	53.8/58.9/61.7

Table S7 The fitting values of components in equivalent circuit for Fig. 7b.

Sample#	Rs (Ω)	Rct-1 (Ω)	CPE-1-T (F)	Rct-2 (Ω)	CPE-2-T (F)	Wo-R (Ω)	Wo-T (s)
C-T500-t2	7.1	30.2	0.01	27.4	4.8E-05	10.5	0.18
C-T570-t0.5	5.4	23.8	0.04	12.8	1.1E-05	2.8	0.05
C-T570-t2	3.2	4.0	0.02	7.5	0.6E-05	1.1	0.03
C-T570-t4	5.7	3.8	0.10	4.3	1.2E-05	1.6	0.04
C-T700-t0.5	5.1	1.0	0.09	9.3	0.9E-05	4.8	0.06
C-T700-t2	5.3	0.7	0.09	11.0	0.7E-05	4.1	0.06

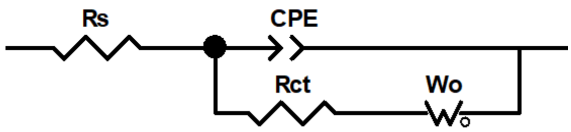

Fig. S11. Equivalent circuit for fitting the Nyquist plot of C-T500-t0.5.

Table S8. The fitting values for C-T570-t0.5 using the equivalent circuit in Fig. S11.

Sample#	Rs (Ω)	Rct (Ω)	CPE-T (F)	Wo-R (Ω)	Wo-T (s)
C-T500-t0.5	4.9	4.1	2.5E-06	4741.0	265.5

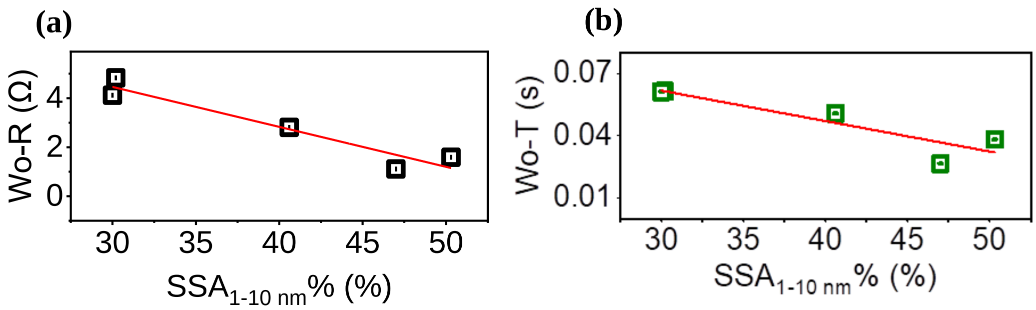

Fig. S12. (a) Wo-R and (b) Wo-T versus the SSA ratio $SSA_{1\text{-}10nm}$% with a fitted trend line in red with the correlation coefficient R^2 ~0.92 and 0.82, respectively.

.